Available online at www.sciencedirect.com
SCIENCE DIRECT
Chemical Physics Letters 417 (2006) 1–5
CHEMICAL PHYSICS LETTERS
www.elsevier.com/locate/cplett

The morphology of thin water films on Pt(1 1 1) probed by chloroform adsorption

G. Zimbitas, A. Hodgson *

Surface Science Research Centre, The University of Liverpool, Oxford Street, Liverpool L69 3BX, UK

Received 30 August 2005; in final form 21 September 2005
Available online 19 October 2005

Abstract

We have investigated water adsorption on Pt(1 1 1) using chloroform to probe the structure and binding sites available on the ice surface. A stable adsorption site appears, associated with growth of ice crystallites on the $(\sqrt{39} \times \sqrt{39})$R16° wetting layer, and disappears slowly as the film grows and loses its registry to the wetting layer. The $\sqrt{39}$ multilayer consists of ordered crystalline ice nuclei which aggregate progressively into a continuous incommensurate ice as the film grows to ~40 layers, the entire film and wetting layer restructuring into an oriented bulk ice only for films more than 50 layers thick.

1. Introduction

Understanding water adsorption and the wetting of metal surfaces is a fundamental problem which underpins many areas of interfacial science [1,2]. This area is attracting renewed interest as detailed experimental and theoretical studies appear which reveal the complexity of water adsorption. On many metal surfaces the water–water hydrogen bond and the water–metal bond have comparable strengths, leading to a subtle balance between optimising the hydrogen bonding interaction in the water layer against the water density and adsorption site on the surface. Water adsorption on Pt(1 1 1) represents a model system which was originally thought to form a simple commensurate hexagonal ice Ih bilayer [1,2], but a much richer picture is slowly emerging, with a complex wetting layer [3–5] influencing the growth of thin films [6,7].

When water is adsorbed on Pt(1 1 1) above ~135 K it forms a series of ordered hexagonal honeycomb structures which interconvert with coverage [3], He diffraction [4] and LEED [5,7] find two highly ordered structures, with extended islands of $(\sqrt{39} \times \sqrt{39})$R25° ice at low coverage which re-arrange and compress as the monolayer is completed to form a $(\sqrt{39} \times \sqrt{39})$R16° structure. Because of the size of the unit cell, the detailed structure of the ice monolayer is not known from experiment. On the basis of STM images [3] it is believed to be a distorted hexagonal honeycomb network of water [4], consistent with a 4% lateral compression of the $\sqrt{39}$ wetting layer compared to bulk ice [4], driven by the increased binding energy of water in contact with the Pt surface. RAIRS spectra [5,6] show little free OH dangling into the vacuum and X-ray absorption measurements [8] are consistent with the majority of water being adsorbed in an H-down configuration. Calculations for a $\sqrt{39}$ monolayer find that water is stabilised compared to simple commensurate $\sqrt{3}$ structures, with a variety of different adsorption geometries which include partially ionised species resembling $OH^{(-)}$ and $H_3O^{(+)}$ embedded within the hydrogen bonded network [9,10]. Simple commensurate $(\sqrt{3} \times \sqrt{3})$R30° structures form only when OH is present to pin the layer into an atop adsorption site, forming a stable mixed $(OH + H_2O)$ structure [11,12].

Continued adsorption results in growth of crystalline ice multilayers on the $(\sqrt{39} \times \sqrt{39})$R16° wetting layer, the multilayer desorbing some 15 K lower in temperature [5,13]. Unlike the large islands formed below one

* Corresponding author. Fax: +44 151 794 3870.
E-mail address: ahodgson@liverpool.ac.uk (A. Hodgson).

0009-2614/$ - see front matter © 2005 Elsevier B.V. All rights reserved.
doi:10.1016/j.cplett.2005.09.127

monolayer, STM images show the second layer nucleating with a high density of small clusters at regular points in the unit cell [3]. Nucleation of the second layer is strongly inhibited, with water uptake accelerating as the second layer is deposited and no further adsorption structure to suggest layer by layer growth [5]. The intensity of the $(\sqrt{39} \times \sqrt{39})$R16° LEED pattern increases as the second layer grows and disappears progressively for films ~10–40 layers thick [6]. Films more than ~50 layers thick restructure the $\sqrt{39}$ wetting layer to form an incommensurate bulk ice Ih(0 0 0 1) film [14] oriented to the Pt(1 1 1) surface. The different ice structures appear reversibly during desorption and crystallisation of amorphous ice, with evidence for roughening of the surface and coexistence of $\sqrt{37}$ islands and $\sqrt{39}$ multilayers after desorption [6].

The steady disappearance of the $\sqrt{39}$ order as the crystalline ice film grows thicker [6] indicates that ice multilayers do not retain a simple epitaxy to the wetting layer, thicker layers forming an incommensurate crystalline ice before the entire film re-crystallises above 50 layers. Here, we investigate how the ice film develops using $CHCl_3$ adsorption as a probe of the local ice structure. Adsorption–desorption of species such as $CHCl_3$ [15–18], CHF_2Cl [19], CCl_4 [20] and N_2 [21], provide a useful means of interrogating the ice surface, giving a fingerprint for changes in the surface morphology and adsorption environment.

2. Experimental

The apparatus used to examine water adsorption–desorption on Pt(1 1 1) has been described in detail previously [5,6]. A Pt(1 1 1) crystal (±0.25°) was attached via Ta heating wires to liquid nitrogen cooled support posts, allowing the crystal to be heated to 1200 K and then cooled to 85 K within a few minutes. Temperature was measured using a chromel–alumel thermocouple spot welded to the side of the crystal and controlled via computer feed back to a DC heating supply. Water and $CHCl_3$ temperature programmed desorption (TPD) were monitored by a QMS mounted directly in front of the sample. Heating rates between 0.25 and 5 K s^{-1} gave consistent results and all data shown here were obtained at 0.5 K s^{-1}. Surface cleanliness was judged from the water TPD and LEED patterns. Water and $CHCl_3$ were dosed using a collimated, effusive molecular beam and the direct reflection technique to monitor adsorption. Crystalline ice films were grown by adsorbing water slowly (typically 0.01 ML s^{-1}) at a temperature of 138 K while amorphous solid water films (ASW) were formed by adsorption at 95 K using a beam at normal incidence. The water coverage was calibrated against the uptake required to complete the $\sqrt{39}$ ice layer on Pt(1 1 1) which is defined as one monolayer (ML). TPD of water and $CHCl_3$ provide a second measure of the coverage and were calibrated against the monolayer desorption peaks. Repeat measurements of the monolayer reference peak reveal an error of ±3% for $CHCl_3$ coverage.

3. Results

Chloroform was first adsorbed on clean Pt(1 1 1) at 95 K and TPD spectra recorded as a function of coverage, Fig. 1. At low coverage a peak (α) appears at ~200 K, which saturates before a second peak (β) appears at ~140 K. These two peaks have similar coverage and saturation of the first peak is defined (arbitrarily) as 1 ML and all coverages normalised to this. At higher coverage a multilayer peak (γ) appears at ~130 K. Chloroform adsorption is stabilised next to the Pt(1 1 1) surface, the second layer being bound slightly more strongly to this than in the multilayer. The second layer peak (β) shifts up slightly in desorption temperature when a multilayer is present to act as a reservoir, repopulating the second layer.

When $CHCl_3$ is dosed onto 5 ML of ASW a single $CHCl_3$ desorption peak is seen near 130 K [22] and grows indefinitely with increasing $CHCl_3$ coverage, Fig. 2a. Desorption is completed before water starts to desorb and the $CHCl_3$ peak is indistinguishable from the multilayer peak (γ) seen on clean Pt(1 1 1), Fig. 1. Fig. 2b shows the effect of changing the ice thickness on desorption of a single layer of $CHCl_3$. For ASW films $\geqslant$2.5 ML only the $CHCl_3$ multilayer peak appears but new features appear near 135 and 145 K as the thickness is decreased below 2.5 ML. There is no evidence for $CHCl_3$ reaching the Pt(1 1 1) surface provided the ASW coverage is above ~1.5 ML.

Chloroform desorption from 5 ML of crystalline ice is shown in Fig. 3 as a function of the initial dose. For low $CHCl_3$ doses (<1 ML) two desorption peaks are found, one near the position of the $CHCl_3$ multilayer and a second peak (δ) near 150 K, which was not present on ASW. This peak occurs in coincidence with the onset of water desorption and has a similar activation behaviour. The presence of $CHCl_3$ does not perturb the ice desorption profiles. Whereas, usually the highest temperature desorption feature (corresponding to the most stable adsorption state) is populated at low coverage, followed by less stable sites

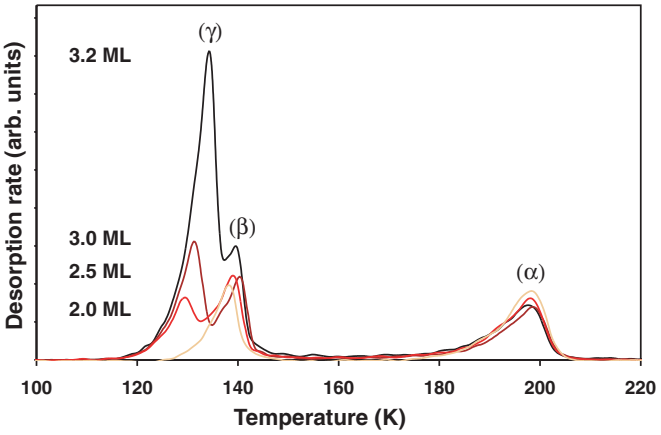

Fig. 1. Chloroform desorption from clean Pt(1 1 1).

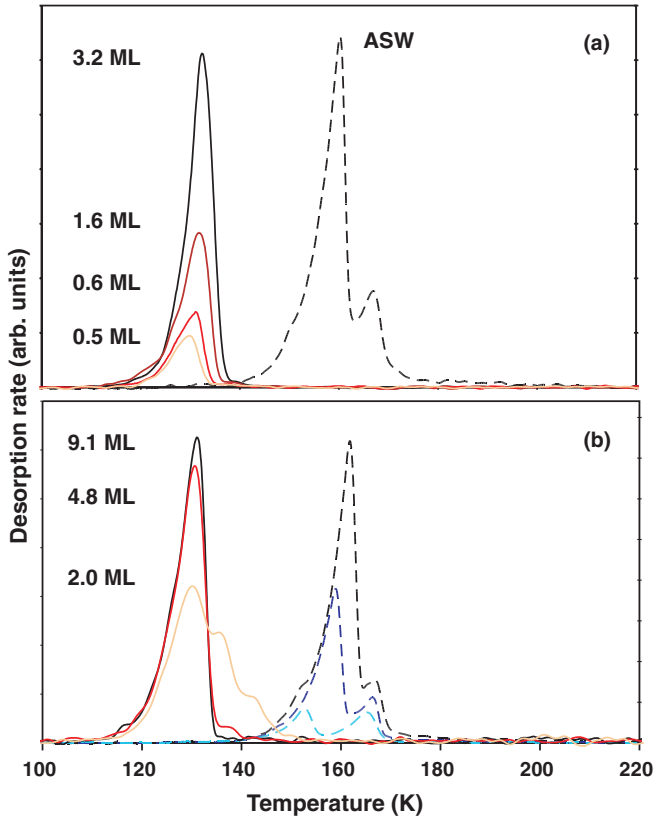

Fig. 2. (a) Chloroform desorption (solid lines) from 5 ML ASW (dotted line) as a function coverage. (b) Desorption of 1 ML chloroform (solid line) from ASW films of different thickness (dashed lines).

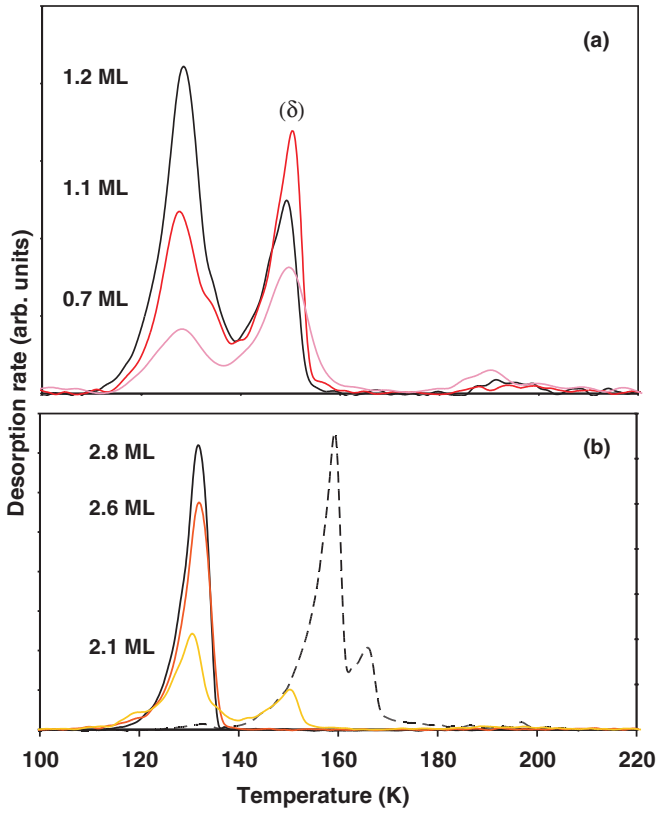

Fig. 3. Chloroform TPD (solid lines) from 5 ML crystalline ice (dotted line) for: (a) low and (b) higher $CHCl_3$ coverage.

at higher coverage (cf. Fig. 1), these two peaks grow simultaneously as the $CHCl_3$ coverage is increased up to 1 ML. This indicates that $CHCl_3$ cannot interconvert from one form to the other and is consistent with a different local environment for adsorption. As soon as the dose is increased above 1 ML the high temperature desorption peak disappears and only the multilayer desorption peak is observed, which continues to grow with the increasing coverage (cf. Fig. 1).

The observation of a single desorption peak for $CHCl_3$ doses above 1 ML indicates that multilayer $CHCl_3$ does not interact sufficiently with the ice surface to probe the different morphology or adsorption sites available. The abrupt change in behaviour suggests that the second layer causes chloroform to form a different structure on the surface, presumably reorienting to the second $CHCl_3$ layer rather than binding to specific sites on the ice surface. This is qualitatively consistent with the expectation that water and chloroform do not mix. Whatever the explanation, the high temperature (δ) peak seen for desorption of <1 ML $CHCl_3$ from 5 ML crystalline ice (but not ASW) provides a probe of the changing structure of the ice film and was previously used to probe the crystallisation of ice on stepped Pt(5 3 3) surfaces [15].

Changes to the surface of crystalline ice films with thickness were followed by adsorbing 1 ML of $CHCl_3$ on top of the ice and recording the desorption spectra, Fig. 4. Films >50 ML have a hexagonal ice Ih(0 0 0 1) LEED pattern while those below ~40 ML show $\sqrt{39}$ spots [6]. For crystalline ice films greater than ~40 ML thick we find only the low temperature multilayer $CHCl_3$ peak, with no desorption above 137 K. As the ice thickness is decreased below ~40 ML the high temperature peak (δ) begins to appear, initially as a weak tail but with increasing intensity to form a distinct peak which follows the water desorption trace for ice films below ~20 ML. As the ice thickness drops to 3–4 ML this peak dominates the desorption profile. This behaviour changes as the ice thickness decreases further, the (δ) peak disappears below 2 ML and is replaced first by multilayer desorption and then by two peaks near 135 and 145 K as the $\sqrt{39}$ wetting layer is exposed. A similar stabilisation is seen for thin ASW films (Fig. 2) and probably relates to the polarisation of the first layer ice [17] (cf. Fig. 1). The appearance of the peak at 200 K indicates that some of the $CHCl_3$ is able to reach the Pt(1 1 1) surface when adsorbed on a single ice monolayer.

4. Discussion

Chloroform desorption shows a peak (δ) at 150 K which is associated only with adsorption on thin $\sqrt{39}$ multilayers, whereas desorption from thick (>40 ML) crystalline ice and ASW films (Figs. 2 and 4) is indistinguishable from

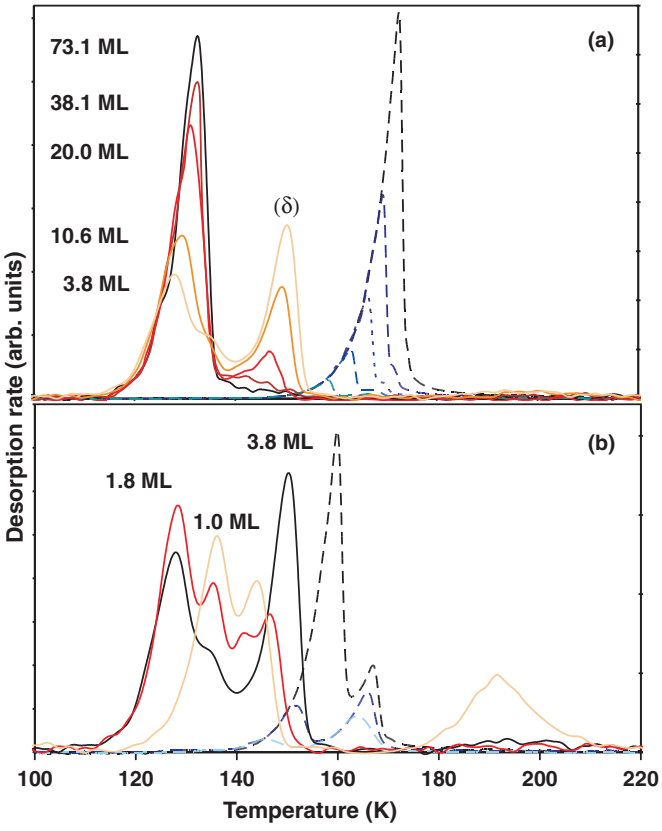

Fig. 4. Change in desorption profile for 1 ML $CHCl_3$ (solid lines) adsorbed on crystalline ice (dotted lines) of different thickness (marked on the left against the respective $CHCl_3$ desorption trace).

multilayer desorption [18]. This is consistent with a weak chloroform–water hydrogen bond [16–18,23] and rules out $CHCl_3$ desorption as a simple diagnostic indicator of the crystallinity of ice surfaces [15,22]. The large ($\Delta T \sim 15$ K) stabilisation of $CHCl_3$ on thin $\sqrt{39}$ crystalline ice multilayers cannot be associated simply with a minor change in the local hydrogen bonding environment or coordination number [23], but reflects a gross change in the ice morphology. In view of the quantity of $CHCl_3$ adsorbed ($\leqslant 0.5$ ML $CHCl_3$ for 4 ML ice) this is attributed to condensation in pores [20,21,24].

The intensity of the (δ) desorption feature (Fig. 4) correlates closely with the intensity of the $\sqrt{39}$ LEED pattern for the ice multilayer [6]. The $\sqrt{39}$ pattern becomes more intense as the first few ice layers are adsorbed on top of the $\sqrt{39}$ wetting layer and then steadily fades as the thickness increases from 10 to 40 ML. This indicates that thin multilayers nucleate in registry with the $\sqrt{39}$ structure, but the film (which RAIRS and desorption indicate is crystalline) then loses its registry to the wetting layer [6]. The chloroform (δ) desorption peak follows a similar pattern, maximising for films ~3–4 ML thick, then weakening as the thickness increases and disappearing above ~40 ML.

STM images show the second layer nucleating as an ordered array of clusters on the wetting layer, rather than as extended islands as on the Pt(1 1 1) surface [3]. Formation of second layer nuclei is inhibited, but ice growth accelerates once these are formed [5] with no indication of any further layer structure either in the water uptake or He scattering [25]. On the basis of LEED experiments [6], we recently proposed that the strain caused by the lateral compression of the $\sqrt{39}$ ice template hinders lateral growth of multilayer clusters which nucleate at particular sites in the $\sqrt{39}$ unit cell (e.g., at ionised sites [9,10]). The lateral periodicity of the crystallites contributes to the intensity of the $\sqrt{39}$ LEED pattern as the multilayer grows. Stabilisation of $CHCl_3$ desorption on these thin films is consistent with adsorption in pores between the multilayer ice crystallites. The disappearance of the (δ) peak with increasing coverage indicates that these start to aggregate above ~3–4 ML, slowly removing the sites at which $CHCl_3$ adsorbs, Fig. 5. This is consistent with the $\sqrt{39}$ LEED pattern starting to fade above this coverage as the $\sqrt{39}$ ice clusters aggregate to form incommensurate ice, attenuating the LEED intensity which originates from ordered structures buried close to the Pt wetting layer [6]. For thick layers >50 ML the entire film restructures, removing the $\sqrt{39}$ wetting layer and relaxing strain in the ice, to create an ordered bulk Ih(0 0 0 1) surface which is oriented to the Pt(1 1 1) surface.

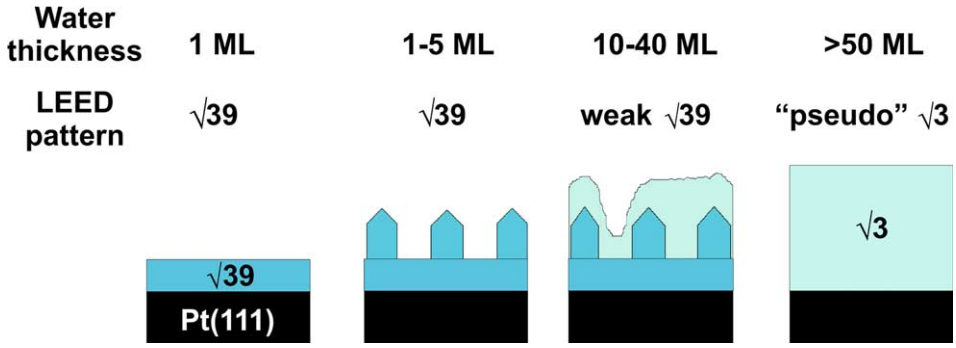

Fig. 5. Cartoon showing the development of multilayer ice structures on Pt(1 1 1) as a function of thickness.

5. Conclusion

Chloroform desorption cannot distinguish between crystalline and amorphous ice, but is sensitive to the gross morphology of thin ice surfaces. A stable $CHCl_3$ adsorption site appears as multilayer ice nucleates in an ordered array of crystallites on the $(\sqrt{39} \times \sqrt{39})$R16° ice template. Correlation of $CHCl_3$ desorption and LEED measurements [6] indicates that aggregation into an incommensurate ice film is only completed as the ice coverage increases to ~40 ML. For thick crystalline ice films the $\sqrt{39}$ wetting layer restructures to form an incommensurate bulk ice Ih(0 0 0 1) film, removing the strain associated with the $\sqrt{39}$ ice/bulk ice interface at the cost of a less optimum water–Pt(1 1 1) interaction.

Acknowledgments

We thank Sam Haq for useful discussion.

Note added in proof

After this paper was submitted we became aware of similar work using Kr adsorption to probe the ice morphology on Pt(1 1 1) [26].

References

[1] P.A. Thiel, T.E. Madey, Surf. Sci. Rep. 7 (1987) 211.
[2] M.A. Henderson, Surf. Sci. Rep. 46 (2002) 5.
[3] M. Morgenstem, J. Muller, T. Mchely, G. Comsa, Z. Phys. Chem. 198 (1997) 43.
[4] A. Glebov, A.P. Graham, A. Menzel, J.P. Toennies, J. Chem. Phys. 106 (1997) 9382.
[5] S. Haq, J. Harnett, A. Hodgson, Surf. Sci. 505 (2002) 171.
[6] G. Zimbitas, S. Haq, A. Hodgson, J. Chem. Phys. 123(13), in press.
[7] J. Harnett, S. Haq, A. Hodgson, Surf. Sci. 528 (2003) 15.
[8] H. Ogasawara, B. Brena, D. Nordlund, M. Nyberg, A. Pelmenschikov, L.G.M. Pettersson, A. Nilsson, Phys. Rev. Lett. 89 (2002) 276102.
[9] S. Meng, E.G. Wang, S.W. Gao, Phys. Rev. B 69 (2004) 195404.
[10] S. Meng, Surf. Sci. 575 (2005) 300.
[11] C. Clay, S. Haq, A. Hodgson, Phys. Rev. Lett. 92 (2004) 046102.
[12] G. Held, C. Clay, S. Barrett, S. Haq, A. Hodgson, J. Chem. Phys. 123 (2005) 064711.
[13] J.L. Daschbach, B.M. Peden, R.S. Smith, B.D. Kay, J. Chem. Phys. 120 (2004) 1516.
[14] N. Materer, U. Starke, A. Barbieri, M.A. VanHove, G.A. Somorjai, G.J. Kroes, C. Minot, Surf. Sci. 381 (1997) 190.
[15] E.H.G. Backus, M.L. Grecea, A.W. Kleyn, M. Bonn, Phys. Rev. Lett. 92 (2004) 236101.
[16] M. Aoki, Y. Ohashi, S. Masuda, Surf. Sci. 532 (2003) 137.
[17] J.E. Schaff, J.T. Roberts, Surf. Sci. 426 (1999) 384.
[18] J.E. Schaff, J.T. Roberts, J. Phys. Chem. 100 (1996) 14151.
[19] D.J. Safarik, R.J. Meyer, C.B. Mullins, J. Vac. Sci. Tech. A 19 (2001) 1537.
[20] V. Sadtchenko, K. Knutsen, C.F. Giese, W.R. Gentry, J. Phys. Chem. B 104 (2000) 2511.
[21] G.A. Kimmel, K.P. Stevenson, Z. Dohnalek, R.S. Smith, B.D. Kay, J. Chem. Phys. 114 (2001) 5284.
[22] M.L. Grecea, E.H.G. Backus, H.J. Fraser, T. Pradeep, A.W. Kleyn, M. Bonn, Chem. Phys. Lett. 385 (2004) 244.
[23] S. Picaud, P.N.M. Hoang, Phys. Chem. Chem. Phys. 6 (2004) 1970.
[24] K.P. Stevenson, G.A. Kimmel, Z. Dohnalek, R.S. Smith, B.D. Kay, Science 283 (1999) 1505.
[25] A. Glebov, A.P. Graham, A. Menzel, J.P. Toennies, P. Senet, J. Chem. Phys. 112 (2000) 11011.
[26] G.A. Kimmel, N.G. Petrik, Z. Dohnalek, B.D. Kay, Phys. Rev. Lett., in press.